



Numerical modelling framework for assessing dune effectiveness against coastal inundation

Italo R. Lopes^{1,2}, Ivan Federico², Michalis Vousdoukas³, Luisa Perini⁴, Salvatore Causio², Giovanni Coppini², Maurilio Milella⁵, Nadia Pinardi^{1,2}, Lorenzo Mentaschi^{1,2}

¹Centro Interdipartimentale di Ricerca per le Scienze Ambientali (CIRSA) - Alma Mater Studiorum Università di Bologna (UNIBO), Ravenna, 48121, Italy

²Centro euro-Mediterraneo sui Cambiamenti Climatici (CMCC), Lecce, 73100, Italy

³MV Coastal and Climate Research Ltd, Limassol, 3046, Cyprus

⁴Servizio Geologico, Sismico e dei Suoli, Regione Emilia-Romagna, Bologna, 40127, Italy

⁵Environmental Surveys S.r.l. (ENSU), Bari, 70125, Italy

Correspondence to: Italo R. Lopes (italo.dosreislopes2@unibo.it)

Abstract. Coastal inundation is one of the prominent natural hazards threatening both economic assets and human lives. Precise modeling of these events is vital for comprehensive risk assessment, yet there is a persistent gap in data availability and modelling accuracy for coastal flood mapping. In this study, we expanded the LISFLOOD-FP model's ability to simulate coastal floods by incorporating wave setup and swash, as well as the interaction with protective infrastructures like temporary dunes. This improved approach was applied to the coastline of Cesenatico, Italy, where dunes are built each winter as seasonal coastal defenses. We analyzed two storm events for which observational flood maps are available for validation: the 2015 Saint Agatha Storm, which saw intense waves breaching the dunes and causing extensive inland flooding, and the 2022 Denise Storm, when the dunes withstood the storm and successfully shielded the coast. Our results demonstrate that dunes are highly effective in mitigating inundation, particularly during the 2022 event. However, they also reveal that the failure of even a small portion of the dunes can lead to widespread inundation, emphasizing the need for optimized dune design. These findings represent a significant advancement toward developing a digital twin of coastal regions, providing valuable support for a range of coastal management activities.

1 Introduction

Floods are substantial environmental hazards that impact global populations and present significant socio-economic challenges (UNODRR, 2020). In Europe, climate-related economic losses between 1980 and 2020 are estimated in 450 to 520 billion euros, with hydrological events being the most impactful (44%) (EEA, 2023). Projected scenarios indicate that coastal flood-related damage could reach up to 1 trillion euros annually by 2100, due to the ongoing climate changes and the related Sea Level Rise (SLR) (European Environmental Agency, EEA, 2024). Climate Change, urbanization and migration



into coastal areas contribute for a rise in coastal exposure (IPCC, 2018) emphasizing the critical importance of accurate representation and effective management of coastal flood events for risk prevention.

35 Flood numerical modeling techniques vary widely, from simple bathtub models (Didier et al., 2019; Williams & Lück-Vogel, 2020), which tend to overestimate flooding, to comprehensive representations of hydro-morphodynamical processes (Vousdoukas, 2012; Wilmink et al., 2023), which require extensive data inputs and computational resources. Intermediate complexity models, solving the shallow water equations for floodplains, such as LISFLOOD-FP (Bates & De Roo, 2000; Bates et al., 2010; Shaw et al., 2021), offer a good balance between accuracy and computational efficiency. Initially
40 developed to extend the LISFLOOD model for river channels and floodplain inundations, LISFLOOD-FP has proven to have skills comparable to more complex hydrological inundation models while using lower computational resources (Smith et al., 2012; Vousdoukas et al., 2016; Bessar et al., 2021). In the European Flood Awareness System (EFAS) project, LISFLOOD-FP is used on a large scale to create datasets of river flood hazard maps by using hydrological data over various return periods to generate flood scenarios (Dottori et al., 2022).

45 LISFLOOD-FP is also a popular choice for coastal flood modelling. Indeed, the European Coastal Flood Awareness System (ECFAS) project (<https://www.ecfas.eu>), relies on LISFLOOD-FP to simulate inundations in the coastal area. The ECFAS project aims to improve flood awareness and preparedness along the European coastline, focusing on the significant economic impacts of coastal flooding. Le Gal et al. (2023) developed comprehensive flood maps generated by LISFLOOD-FP for different coastal sectors on the European coasts, considering synthetic scenarios that provide general insights into
50 flood hazard assessment across Europe. However, local-scale coastal studies highlight the limitations in our capabilities to predict this phenomenon. To start, accurate coastal flood modelling requires accurate data of Total Water Level (TWL), which consists of Sea Surface Height (SSH) and wave components, to accurately represent flood extent (Zhang & Najafi, 2020; Carneiro-Barros et al., 2023). This implies that LISFLOOD-FP offshore lateral open boundary conditions must include information as accurate as possible on sea level and waves.

55 Another modelling limitation discussed by Dottori et al. (2022) and Carneiro-Barros et al. (2023) is the non-inclusion of defenses in the simulations. Coastal defenses encompass a range of structures, including hard engineering solutions, Nature-Based Solutions (NBS), and hybrid forms that vary in structural complexity and interaction with storm events (Almarshed et al., 2020). Incorporating these defensive structures into numerical models poses a challenge, as accurate representation requires detailed information on defense geometries and potential modifications in response to flooding. Coastal dunes, a
60 form of NBS commonly found on sandy shorelines, provide effective protection against storm surge-induced flooding by acting as barriers near the beach interface (Singhvi et al., 2022; Wijnberg et al., 2021). However, the numerical modeling of dune erosion presents complex challenges due to the combined effects of storm surges and wave overwash (van Wiechen et al., 2023).

The Italian region of Emilia-Romagna (ER) is an example of a low-lying area vulnerable to coastal flood events usually
65 associated with a combined effect of surge, tides, and waves. Several studies account for the economic losses (Carisi et al., 2018; Armaroli et al., 2019) and hazard assessment impact (Ciavola et al., 2007; Martinelli et al., 2010; Armaroli et al.,



2012). To reduce the hazard, temporary dunes are erected as coastal defenses in November and maintained during the Winter until April. Harley & Ciavola (2013) conducted risk assessments studies related to these seasonal dunes and propose a GIS based methodology for engineering the dunes' geometry. In flood modeling, these dunes present two main challenges: a) accurately representing their elevation and spatial distribution in the topographic data, and b) understanding and modeling their potential responses, including structural failures, during extreme events.

Enhancing our coastal flood modeling capabilities is a critical step toward developing a digital twin for sustainable coastal management. Digital twins are advanced virtual replicas of the physical systems, enabling scenario simulations and exploration while using observational data to continuously refine and calibrate models. Although initially popular in the industrial sector, digital twin technology has recently been adopted for environmental applications across Europe (Nativi et al., 2020). As an example, in Emilia-Romagna Pillai et al. (2022) explores this concept, highlighting the potential of digital twins to improve understanding of wave attenuation through Nature-Based Solutions such as seagrass in the region offshore the coasts. The development of an accurate coastal flood numerical model would enable the exploration of what-if scenarios with the aim of developing an optimal layout of coastal defenses.

To address these gaps, here we introduce novel approaches tailored to parametrize the dynamics of coastal protections and wave component within the LISFLOOD-FP model. Specifically, we incorporate dune structures and a Failure Water Depth (FWD) threshold to simulate their collapse and introduce the effect of wave swash on erosion and on flood water supply.

Our developments were tested by carrying out simulations for two flood events in Cesenatico (Emilia-Romagna, ER) for which observed flood maps are available, provided by the Geological, Seismic and Soil Service of the ER region. The first is the Saint Agatha Storm, which occurred in February 2015. During this event, a significant portion of the artificial dunes along the coast failed resulting in a major flood (Perini et al., 2015). The second event is the Denise Storm, which took place in November 2022, causing a combination of surge, tides and waves that led to floods in part of the region, however in this case the artificial dunes provided an effective protection in large swaths of the coasts.

In section 2 the numerical modelling improvements for the Total Water Level are described, including the Swash boundary forcing, the dune failure assumptions and all the input data used. In section 3 we show the numerical simulations with and without dunes during the two flood events and section 4 concludes with a discussion.

2 Methods and data

2.1 Contribution of waves to coastal water levels

Waves contribute in a complex way to Total Water Levels (TWL), which is defined as the combination of tides, surge, and wave runup (composed by the wave setup and swash). The wave setup associated with the wave dissipation and the related decrease in radiation stress, provide a neat contribution to the coastal sea level (e.g. Melet et al., 2018). The swash is the intermittent water wash-up on the beach as the waves finally break. Although the swash has no effect on the mean sea



level, it contributes to coastal hazard and inundation in at least 2 ways: 1) in extreme conditions the runup is a major driver of erosion, possibly contributing to the collapse of coastal defenses like sandy dunes. 2) A continuous overwash can provide a substantial water supply for coastal inundation compared to mean coastal sea level.

LISFLOOD-FP model domain starts from the coastline that is considered the open boundary condition for Total Water Level (TWL). It then extends on the land as far as necessary. Here we improved the parameterization of the contribution of waves introducing the swash (S) in the TWL, estimated consistently with existing literature (e.g. Stockdon et al., 2006) as the sum of the water level plus half the swash

$$TWL = WL + \frac{S}{2} \quad (1)$$

where the term WL is assumed to contain all the contribution to mean coastal sea level, including the wave setup. TWL is then used in the model to parameterize the possible collapse of coastal defenses (see section 2.2). Furthermore, we considered the contribution of waves to water supply for inundation by introducing the concept of Supply Total Water Level (STWL) (Figure 1), given by:

$$STWL = WL + \frac{\alpha}{2} S \quad (2)$$

where $\alpha \in [0,1]$ is a calibration factor which represents the overwash efficiency. A value of $\alpha = 0$ implies that the contribution of waves is limited to the wave setup, which could lead to an underestimation of the water supply driving the flood, as the overwash effect would be ignored. Conversely, $\alpha = 1$ assumes that the swash continuously contributes to the water supply, disregarding the intermittent nature of overwash and potentially resulting in an overestimation of the water supply.

In our model configuration, the WL is considered as the contribution of the Sea level component due to atmospheric forcing (surge) (SSH_s), Tides (T) and the wave setup $\langle \eta \rangle$

$$WL = SSH_s + T + \langle \eta \rangle \quad (3)$$

The wave-induced contributions were estimated using the approach suggested by Stockdon et al. (2006), which states that the wave setup and swash for waves perpendicular to the coast is given by

$$\langle \eta_0 \rangle = 0.35 \beta_f (HL)^{1/2} \quad (4)$$



$$S_0 = [HL(0.563\beta_f^2 + 0.004)]^{1/2} \quad (5)$$

where $\langle \eta_0 \rangle$ and S_0 are the wave setup and swash assuming a wave propagation perpendicular to the shore, β_f is the beach face-slope which is the inclination of the beach portion between the high tide and low tide lines, H is the Significant Wave Height, L is the mean wavelength. According to Stockdon et al. (2006), the values of $\langle \eta_0 \rangle$ and S_0 are further multiplied by a 1.1 factor, which is the regression coefficient between $\langle \eta_0 \rangle + \frac{S_0}{2}$ and the observed wave runup. Considering waves directed with an angle θ relative to the shoreline, the wave setup and swash set as boundary condition in LISFLOOD-FP in this study is given by

$$\langle \eta \rangle = 1.1 \cdot \max(\sin \theta, 0) \langle \eta_0 \rangle \quad (6)$$

$$S = 1.1 \cdot \max(\sin \theta, 0) S_0 \quad (7)$$

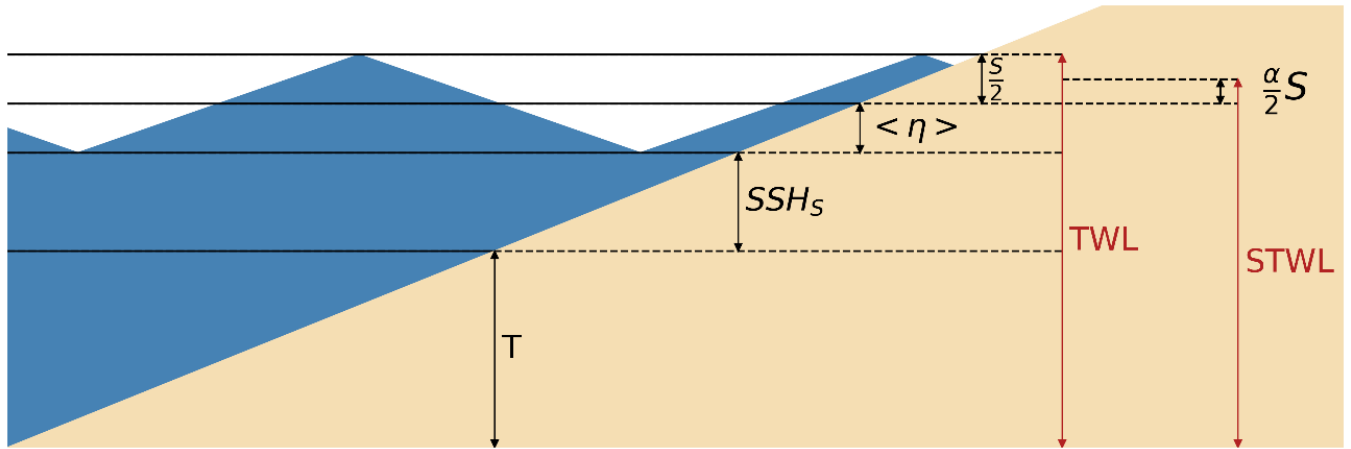


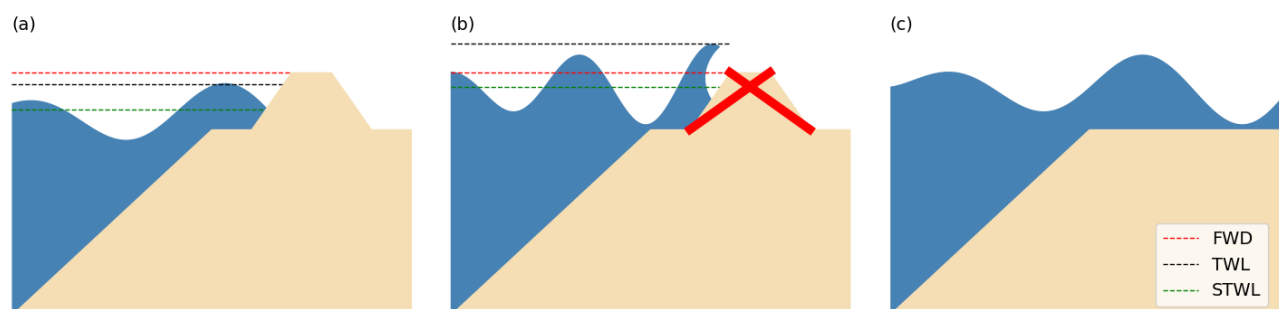
Figure 1: Schematics of the ocean components for the water level and the water supply associated with the swash where T is the tide component, SSH_s is the Sea Surface Height due to surge, $\langle \eta \rangle$ is the wave setup, S is the swash, α is the overwash efficiency, TWL is the Total Water Level and STWL is the Supply Total Water Level.

2.2 Coastal defense structure modelling

The approach proposed in this study takes inspiration from Shustikova et al. (2020), who proposed a methodology for the levee's representation and their breaching. It consists of adding protective, sometimes non-permanent features such as dunes to the DTM, allowing the model to reproduce their effect in blocking the water flow (Figure 2). For each time step, the Total Water Level (TWL) in the vicinity of the dune is compared with its Failure Water Depth (FWD), that is a threshold for dune erosion (e.g. van Rijn, 2009). When the FWD is exceeded, the dune is entirely eroded and removed from the terrain.



140 For the sides of the dune facing the offshore, the FWD is compared to the full TWL, and not the STWL, as the swash plays a prominent role in dune erosion.

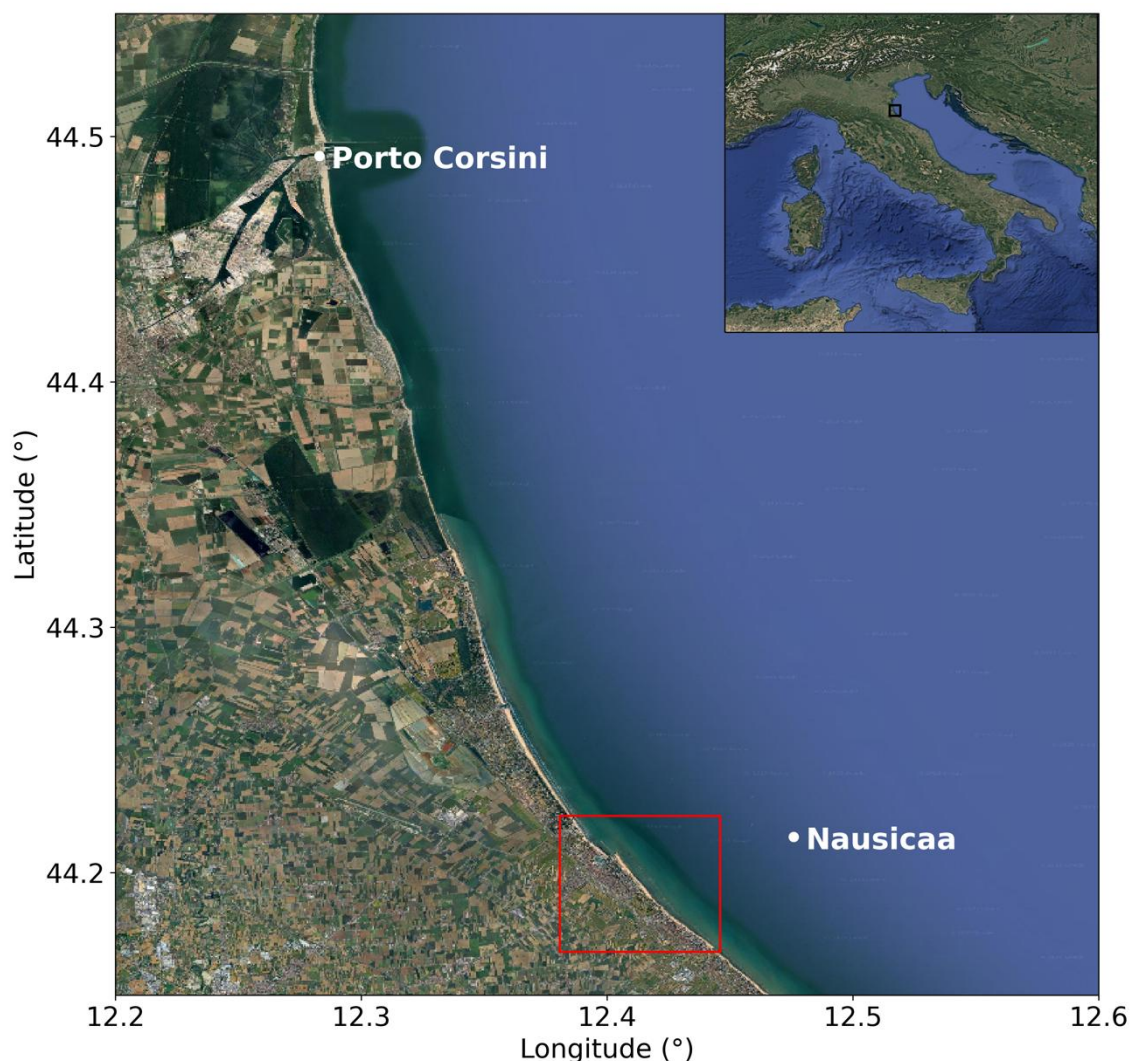


145 **Figure 2: Schematic representation of coastal protections in LISFLOOD-FP. (a): protective action when $TWL < FWD$. (b): failure for $TWL > FWD$. (c) free flood propagation upon protection failure. Red line represents the FWD, black line the TWL and green line the STWL.**

2.3 Model setup and input data validation

150 Among the numerical schemes available in LISFLOOD-FP we selected the acceleration scheme, which offers a trade-off between accuracy and computational parsimony. The model requires lateral boundary conditions for TWL at the coastline, Digital Terrain Model (DTM) data and dune's position/geometry. The TWL, defined in (1), is the combination of sea level and wave data from a large-scale model. These data are provided by the hindcast of Mentaschi et al. (2023), which attains a resolution of 2-4 km along the global coast.

155 Prior to carrying out simulations, we validated the hindcast data for the years 2015 and 2022. We compared the modeled Sea Surface Height (SSH) from Mentaschi et al. (2023) with the data from the tidal station in Porto Corsini, provided by the Istituto Superiore per la Protezione e la Ricerca Ambientale (ISPRA), and the Significant Wave Height (SWH) with the data of the Nausicaa buoy, provided by the Agenzia Regionale per la Prevenzione, Ambiente Energia dell'Emilia-Romagna (ARPAE) (Figure 3).



160 **Figure 3: Emilia-Romagna's coast in the northeast of Italy. White dots represent Porto Corsini's tide gauge (north) and Nausicaa's**
 165 **wave buoy (south). Red rectangle represents the modeled area in the town of Cesenatico. © Google Maps**

To compare Porto Corsini tide gauge data with the model simulation of Mentaschi et al. (2023), which does not include tidal information, the Porto Corsini tide gauge data had to be filtered from the tidal signal. A quasi-daily residual tidal-like signal is still evident in the time series of Figure 4, likely due to the seiches, which in the Adriatic Sea have a period of roughly 22 hours (Medvedev et al., 2020). Visually the comparison is very good, quantitatively the correlation between the hindcast and observed data is 95%, and the RMSE is 0.02 meters for 2015. In 2022, the correlation is 85%, and the RMSE is 0.02 meters.



Regarding wave data, we limited our comparison of Significant Wave Height (SWH) to the year 2015, as the data for 2022 were unavailable from the Nausicaa buoy. The correlation is 97%, with a negative significant wave height BIAS of -0.04 meters and an RMSE of 0.02 meters (Figure 5). These results, show that we can reasonably assume the hindcast provides a reliable representation of the study area and is suitable for use as input data in the model.

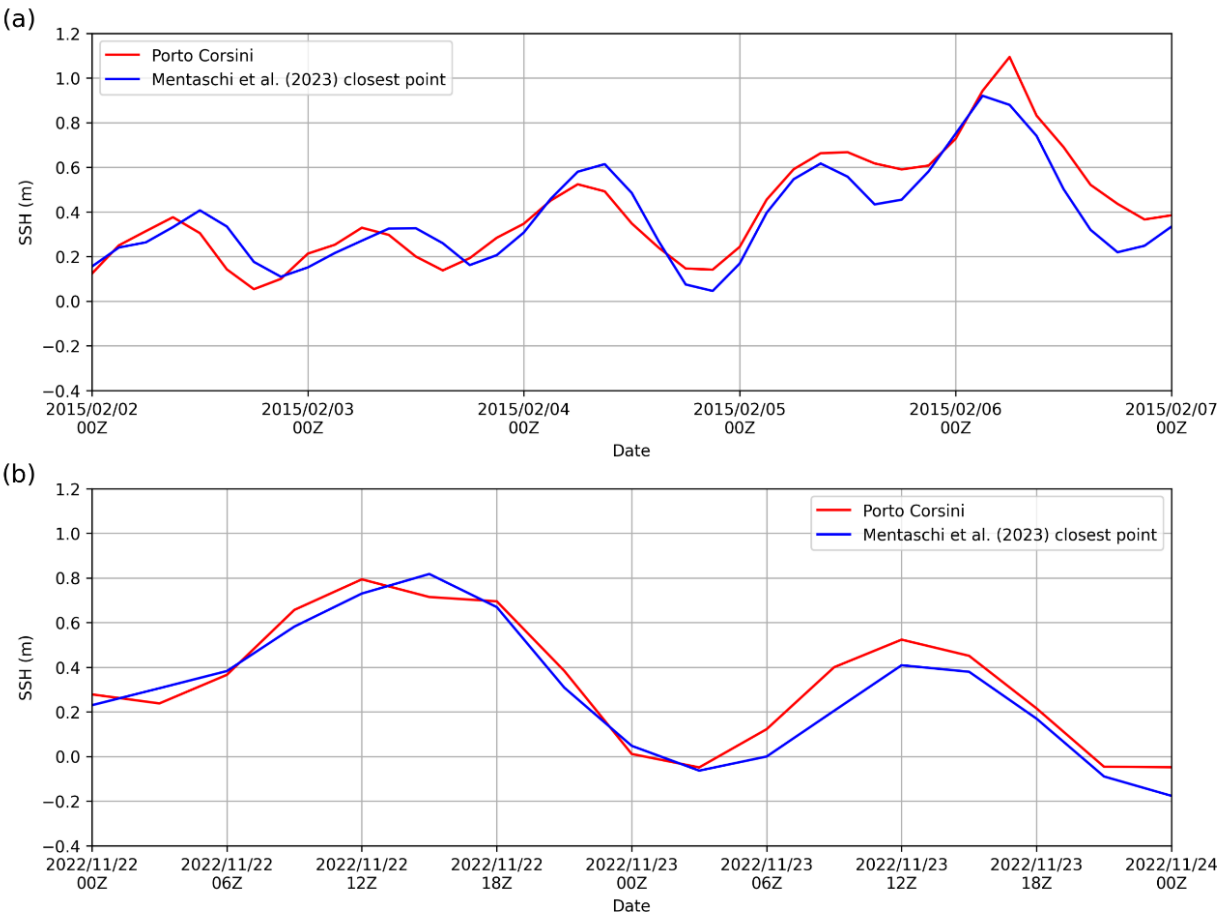


Figure 4: Comparison between the data of storm surge from Mentaschi et al. 2023 (blue line), with the filtered SSH data observed at the Porto Corsini station (red line) for the 2015 event (a) and 2022 event (b).

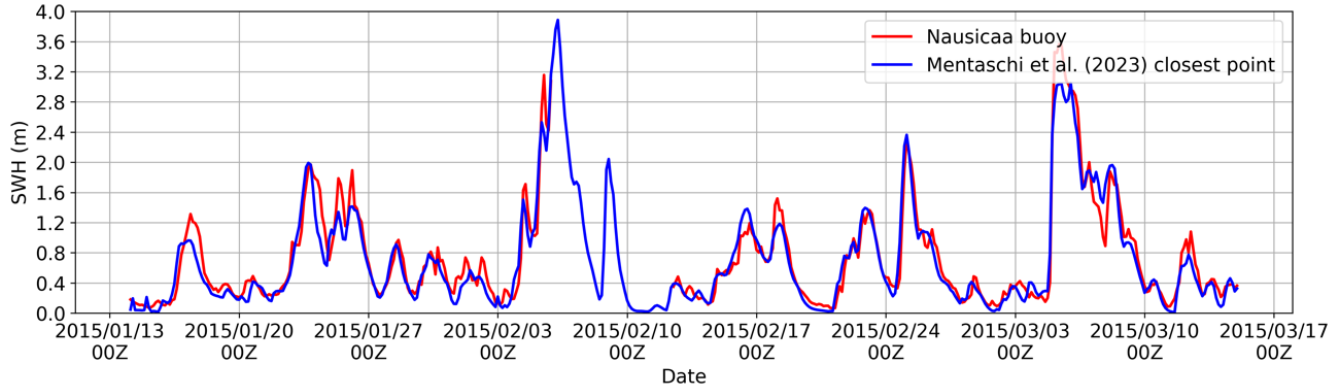
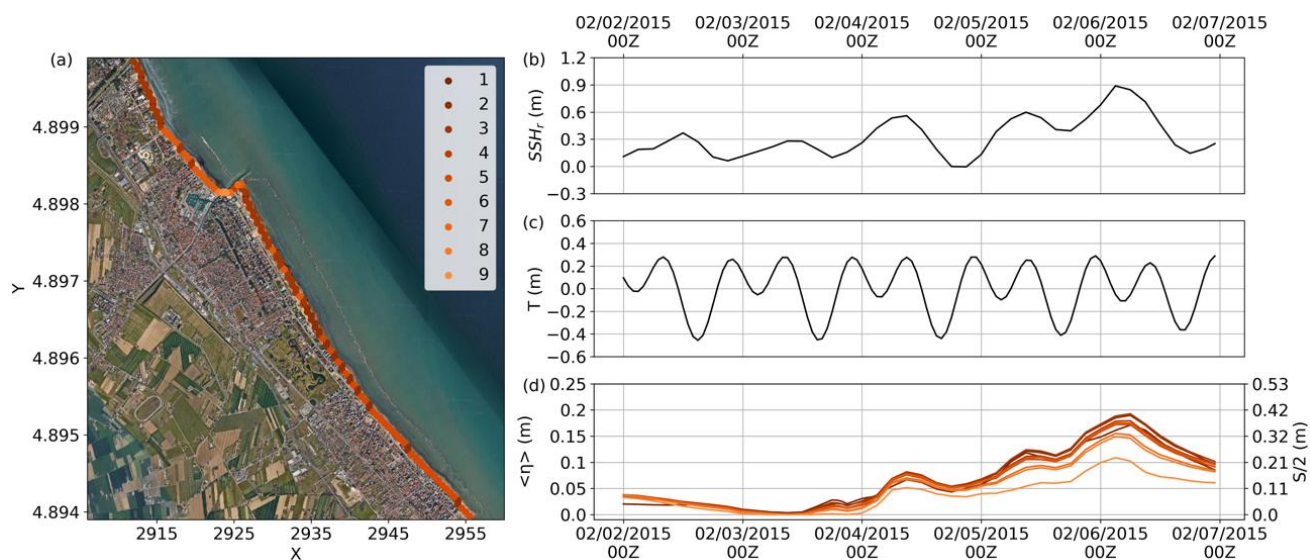


Figure 5: Timeseries of SWH for the Nausicaa buoy (red line) and from Mentaschi et al. 2023 (blue line) for the 3-month event centered comparison in 2015.

180 The DTM was provided by the Geological, Seismic and Soil Service of the ER region. A coastline mapping was carried out to provide boundary points coordinates in the sea/land interface. The coastline is determined by analyzing the DTM, identifying the zero-crossing, and designating the first positive point as its location. The model was set on a domain covering the area of Cesenatico with a resolution of 50 m. The resulting grid has a size of 150x121 grid cells.

For the simulations in Cesenatico (ER), a mapping of the seasonal dunes in the area was carried out from satellite
185 imagery to provide the structures' coordinates. The dunes are, then, positioned in the closest DTM point acquiring a width and length with the same resolution. Moreover, the dunes were all assigned a FWD of 1.4 meters.

The boundary conditions were generated using SSH_r and wave components from the hindcast's closest node, the tide component T from Porto Corsini and the coastline angle. To compute the TWL written in (1), the beach-face slope for the study area was set to $\beta_f = 0.05\%$ according to Ciavola et al. (2006) and the overwash efficiency was set to $\alpha = 0.25$ based
190 on geometrical considerations, and approximating the waves as triangular (Figure 1). With this configuration, 9 different boundary conditions points are obtained along the coast (Figure 6a). The boundary conditions for 2015 and 2022 for the different points are, then, presented in Figure 6 and Figure 7, respectively.



195 **Figure 6: Boundary condition points associated with coastline angle along the Cesenatico area (a). Darker (lighter) colors indicate a more meridional (zonal) coastline orientation (from Google Maps). Panels (b–d) show the boundary conditions for SSHr (m) (b), T (m) (c), and both $\langle \eta \rangle$ (m) and S/2 (m) (d) during the 2015 event. In panel (d), $\langle \eta \rangle$ and S are proportional; the left y-axis corresponds to $\langle \eta \rangle$, while the right y-axis represents S/2, allowing both quantities to be conveyed by a single curve. © Google Maps**

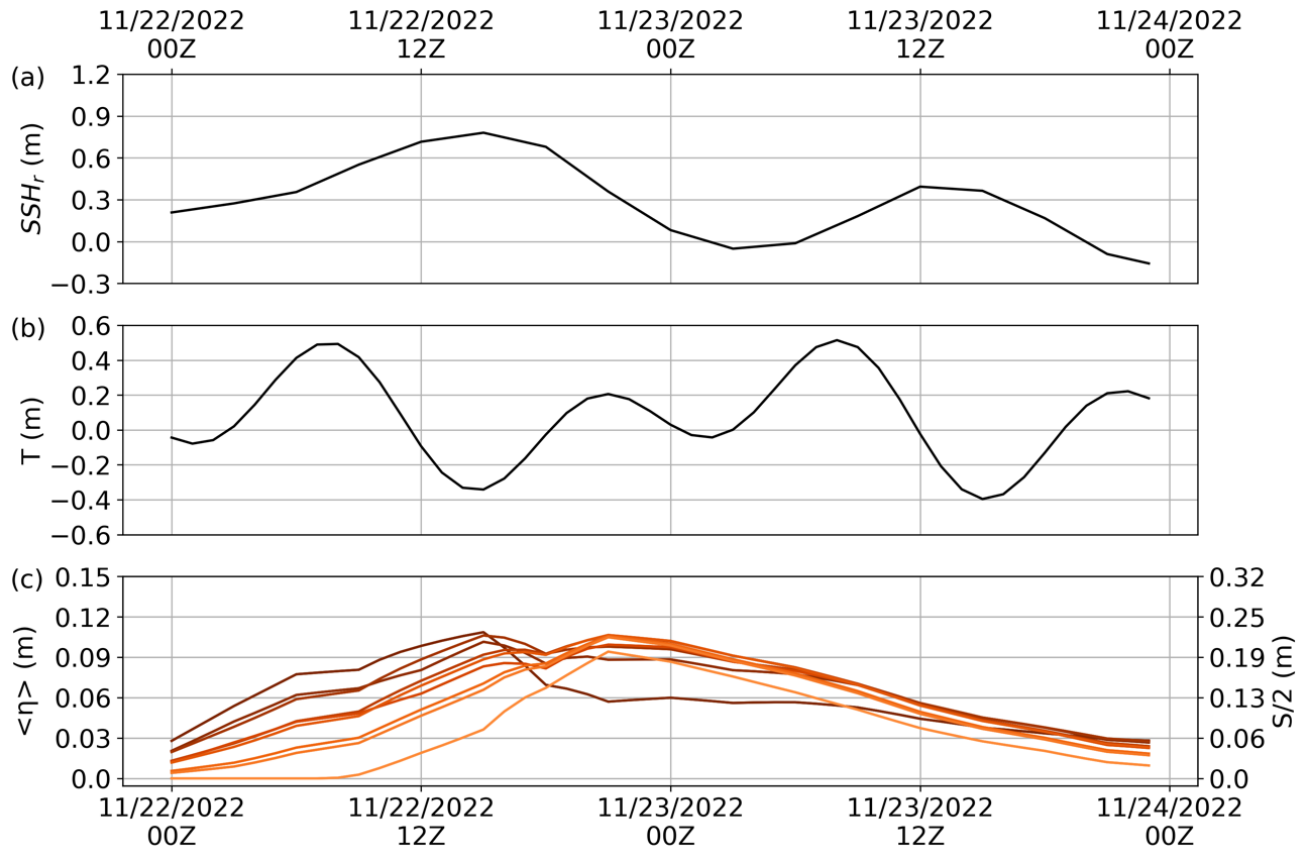


Figure 7: Boundary conditions for SSHr (m) (a), T (m) (b), and both $\langle \eta \rangle$ (m) and S/2 (m) (c) during the 2022 event. In panel (d), $\langle \eta \rangle$ and S are proportional; the left y-axis corresponds to $\langle \eta \rangle$, while the right y-axis represents S/2, allowing both quantities to be conveyed by a single curve. Darker (lighter) colors indicate a more meridional (zonal) coastline orientation.

205

2.4 Simulation experiments and validation

Table 1 contains the description of the numerical experiments. The simulations were carried out for two specific flood events: the storm Agatha of 2015 (from February 2 to February 6, 2015) and the storm Denise of 2022 (from November 22 to November 23, 2022). To understand the dune's contribution to the flood, for each event, 2 simulations were carried out: one without (E2015 and E2022) and one with (E2015D and E2022D) dunes.

Moreover, to understand the waves' contribution to the flood, simulations were carried out by neglecting the contribution of the swash (E2015DWL and E2022DWL) and assuming that waves fully contribute to both dune failure and water supply, by setting a boundary condition equal to TWL (E2015DTWL and E2022DTWL).

Furthermore, we estimated how uncertainty in the DTM propagates in the results of the flood model. Duo et al. (2018) quantified the uncertainty in beach profiles by comparing the measurements of two different instruments in post-storm



conditions after the 2015 event. The Root Mean Square Error (RMSE) between these instruments was found to be 0.12-0.14 meters. Assuming our DTM exhibits a similar range of uncertainty, we conducted additional simulations by adding or subtracting a confidence value of 0.07 m to the DTM. These simulations were performed both with dunes (E2015D+, E2015D-, E2022D+, E2022D-) and without dunes (E2015+, E2015-, E2022+, E2022-), where the +/- suffix indicates the addition or subtraction of the confidence value. We then estimated the uncertainty associated with dunes (UDUNE2015 and UDUNE2022), waves (UWAVE2015 and UWAVE2022) and DTM (UDTM2015 and UDTM2022) as the difference between simulations (Table 2).

Table 1: Simulations configurations using different dunes, lateral boundary conditions, DTM offset and simulation period.

Simulations	Dunes	Dune’s failure condition	Boundary condition	DTM offset	Simulation period	
E2015	No	None	STWL	0 m	02/02/2015 00:00:00 to 06/02/2015 23:00:00	
E2015D	Yes	TWL		0 m		
E2015D+				+ 0.07 m		
E2015D-				- 0.07 m		
E2015DWL	Yes	WL	WL	0 m		
E2015DTWL		TWL	TWL			
E2022	No	None	STWL	0 m		23/11/2022 23:00:00 to 06/02/2015 23:00:00
E2022D	Yes	TWL		0 m		
E2022D+				+ 0.07 m		
E2022D-				- 0.07 m		
E2022DWL	Yes	WL	WL	0 m		
E2022DTWL		TWL	TWL			

Table 2: Uncertainties definition as the difference between simulations.

Uncertainty	Simulations
UDUNE2015	(E2015D) - (E2015)
UDUNE2022	(E2022D) - (E2022)
UDTM2015	(E2015D+) - (E2015D-)
UDTM2022	(E2022D+) - (E2022D-)
UWAVE2015	(E2015DTWL) - (E2015DWL)
UWAVE2022	(E2022DTWL) - (E2022DWL)



The maximum flood extension simulated by LISFLOOD-FP was compared with the observations for each event. The grid points where the model reproduced water levels lower than 10 cm were neglected. For the comparison, the set of skill indicators suggested by Vousdoukas et al. (2016) was used:

- The BIAS is defined as the percentage ratio between predicted and observed area, and values lower (higher) than 100% indicate an underestimation (overestimation) of the flooded area. It is given by

$$BIAS = 100 \times \frac{F_m}{F_o} \quad (8)$$

where F_m and F_o are the extent of the modelled and observed flooded areas.

- The false alarm F is the percentage ratios between wrongly inundated pixels and the observed ones. High values of this indicator indicate a high amount of wrongly inundated areas.

$$F = 100 \times \frac{F_m \neg F_o}{F_o} \quad (9)$$

where $F_m \neg F_o$ indicates the extent of the area flooded in the model but not in the observations.

- The hit ratio (H) provides the opposite information with respect to F , which is an indication on the degree of agreement between the correctly modelled and the observed flooded areas. It is defined as the percentage ratio between the intersection of the modelled/observed flooded areas ($F_m \cap F_o$) and the observed flooded area.

$$H = 100 \times \frac{F_m \cap F_o}{F_o} \quad (10)$$

- The critical success index (C) is a renormalization of H that results in the penalization of the indicator in case of high false alarm. It is defined as the percentage ratio between the intersection of the modelled/observed flooded areas ($F_m \cap F_o$) and the union of the two ($F_m \cup F_o$).

$$C = 100 \times \frac{F_m \cap F_o}{F_m \cup F_o} \quad (11)$$

3 Results

3.1 Effects of dunes in inundation



In Figure 8, the maximum flooded area roughly corresponds with the observed one (cyan line) for the 2015 event. The simulations with and without dunes (E2015D and E2015) are in substantial agreement and reproduce a major coastal
250 flood. However, the simulations show overestimation with a broader flood inland for the whole area except in the south. For E2015 (Figure 8a), the maximum water depth presents lower values in the northern and southern portions of the domain (0.7 meters, in general) and higher values in the center (>1.0 m), with a maximum of 1.18 m. In E2015D (Figure 8b), the high TWL resulted in the failure of the artificial dunes in 7 cells of the domain (5% of all the dunes). Even with the collapse of
255 one of the simulations without protections and water depths 0.03 m smaller.

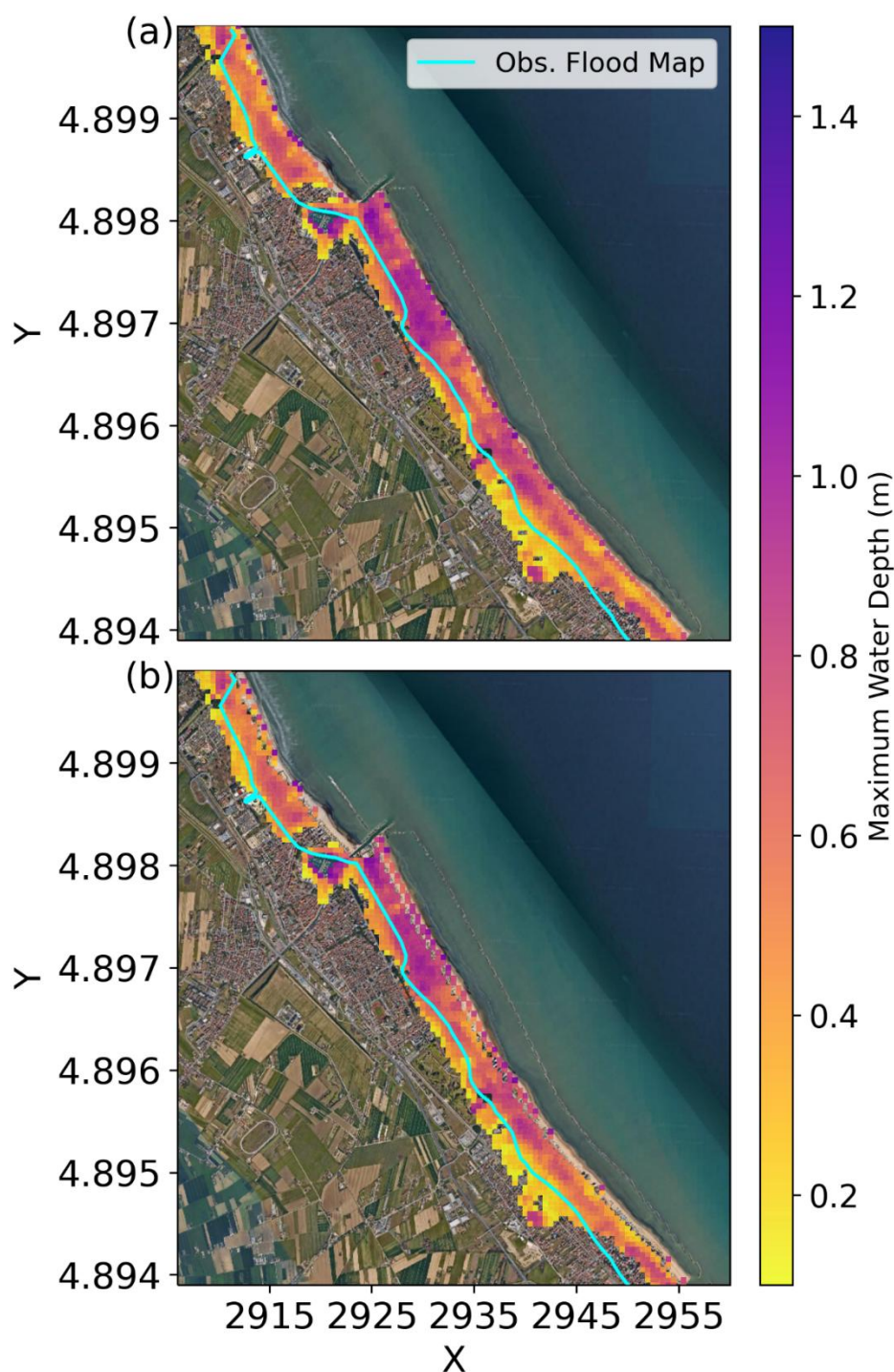


Figure 8: LISFLOOD-FP maximum water depth (m) for the 2015 simulation without protections E2015 (a) and with protections E2015D (b). The cyan line corresponds to the limits of the observational flood area. © Google Maps



260 In terms of evaluation indices (Table 3), the E2015 shows a 132% value of BIAS and 39% value of F, due to the false alarm associated with some overestimation of the event. The simulation also exhibits a 92% value of H and 66 % value of C showing a good representation of the flood extent even with misalignments between the flooded areas. Results for E2015D present similar pattern. Values for BIAS (130%), F (43%), H (88%) and C (59%) indicates that both simulations can similarly reproduce the flood.

265

Table 3: Evaluation metrics for simulations E2015, E2015D, E2022 and E2022D.

Metrics	E2015	E2015D	E2022	E2022D
BIAS (%)	132	130	739	72
F (%)	39	43	640	5
H (%)	92	86	99	67
C (%)	66	60	13	64

270 For the storm Denise of 2022, the simulation without protections (E2022) results in a maximum flood extent larger than the observed one, as the latter includes only areas in the proximity of the shoreline (Figure 9a). In E2022 the flood pattern is like the event of 2015, with a maximum water level lower in the northern and southern portions of the domain (around 0.5 meters) and higher for the central part of the study area (around 0.8 meters). The highest value reached is 1.09 meters. However, the realistic case with dunes (Figure 9b) shows the much-reduced flood extent, consistent with observations (simulation E2022D). This time the dunes did not erode, and their protective action was evident.

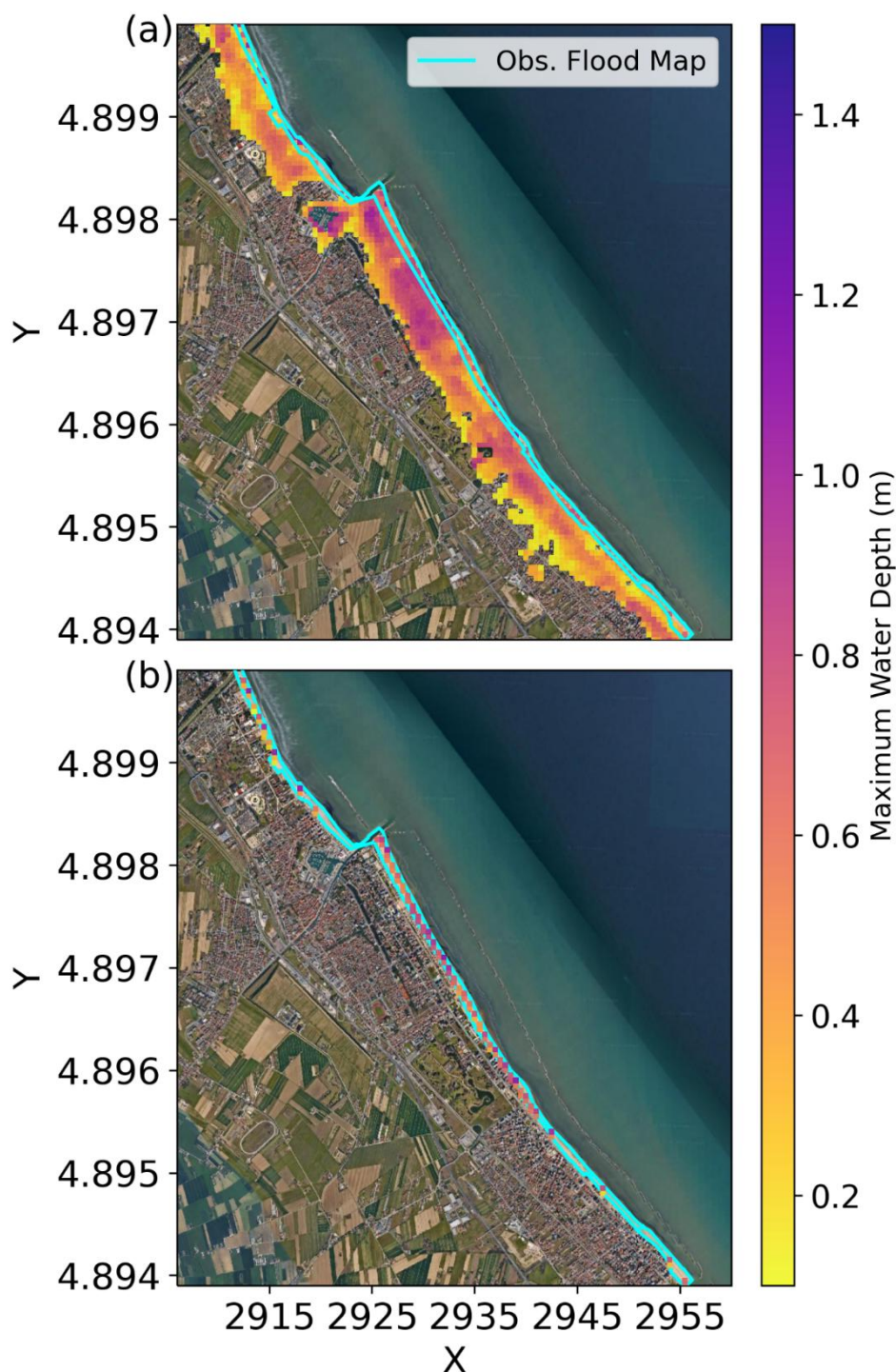


Figure 9: LISFLOOD-FP maximum water depth (m) for the 2022 simulation without protections E2022 (a) and with protections E2022D (b). The cyan line corresponds to the limits of the observational flood area. © Google Maps

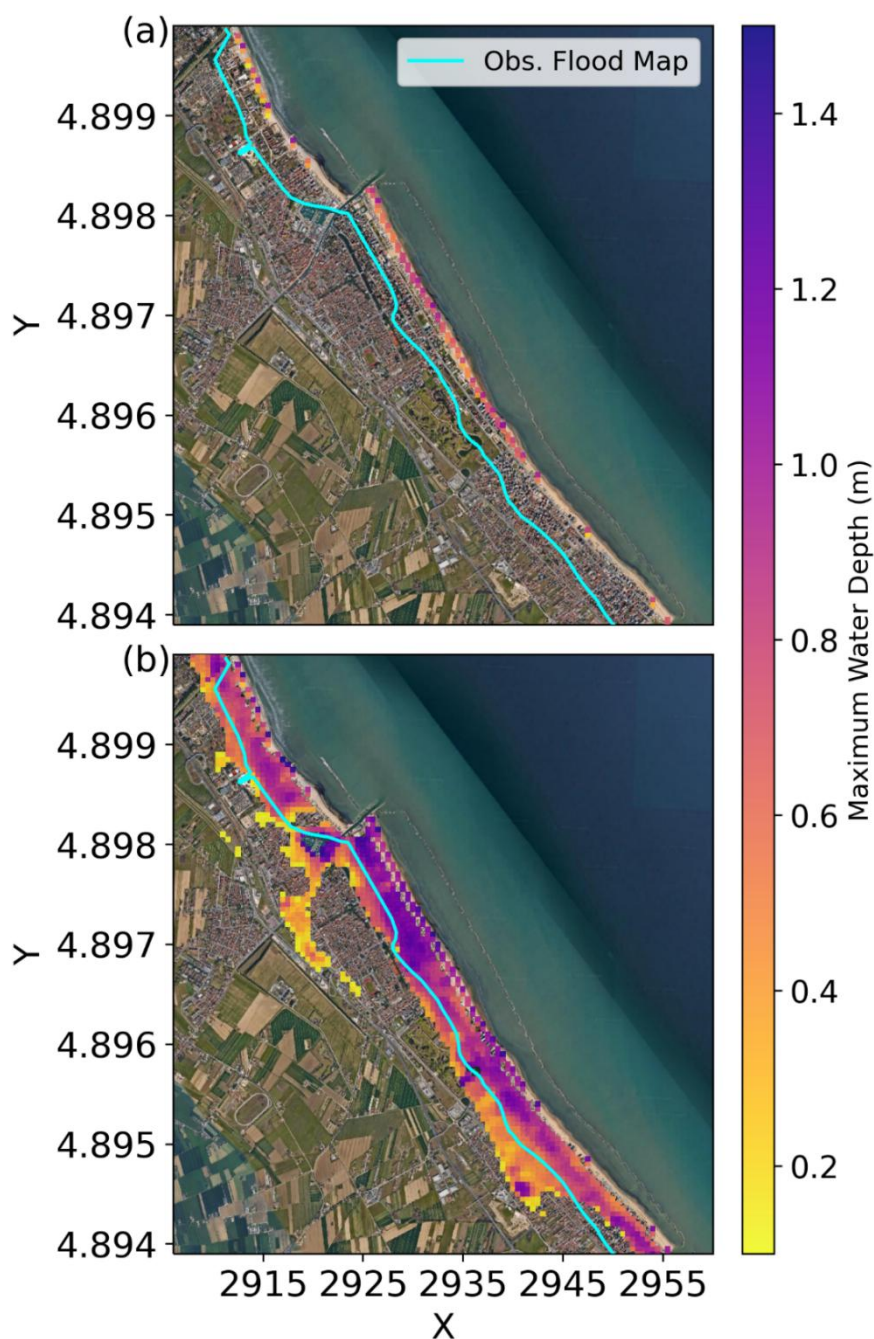


280 The evaluation indices of E2022 display values of 640% of F and 739% of BIAS due to the large overestimation in
maximum flood extent (Table 3). The H value of 99% indicates that most of the cells identified as flooded in the
observations are flooded also in the simulation, but the value of C of 13% indicates that the simulation results in many false
positives. These values are much improved in the simulation with coastal protection (E2022D), where the flooded area
broadly coincides with the observational one. In particular, the false alarm rate drops to 5 %, and the values of BIAS, H and
285 C are reasonable, considering that the width of the flooded area is comparable with the resolution of the model.

3.2 Effects of swash on dune failure

Suspendisse a elit ut leo pharetra cursus sed quis diam (Smith et al., 2014; Miller and Carter, 2015). Nullam dapibus, ante
290 vitae congue egestas, sem ex semper orci, vel sodales sapien nibh sed lectus. Etiam vehicula lectus quis orci ultricies
dapibus. In sit amet lorem egestas, pretium sem sed, tempus lorem.

As discussed in the previous section, during the 2015 event, dune failure occurred not preventing the large
inundation. A correct representation of the waves' contribution is important for the event since dune failure depends on that.
Simulation E2015DWL (Figure 10a), which does not consider the contribution of swash, does not result in dune failure, and
295 reproduces as inundated only tiny areas near the shoreline. By contrast, E2015TWL (Figure 10b), which considers the full
TWL as boundary condition overestimates the flood with a 18% larger maximum flooded area compared with E2015D and
is associated with water depths 0.3 m higher. Thus, we conclude that for the correct reproduction of the dune failure the
contribution of the swash in TWL is important.



300 **Figure 10: Waves' contribution to flood: simulation E2015DWL which does not consider the contribution of swash (a) and simulation E2015TWL which considers the full extent of TWL as contributing to both dune failure and water supply (b). © Google Maps**

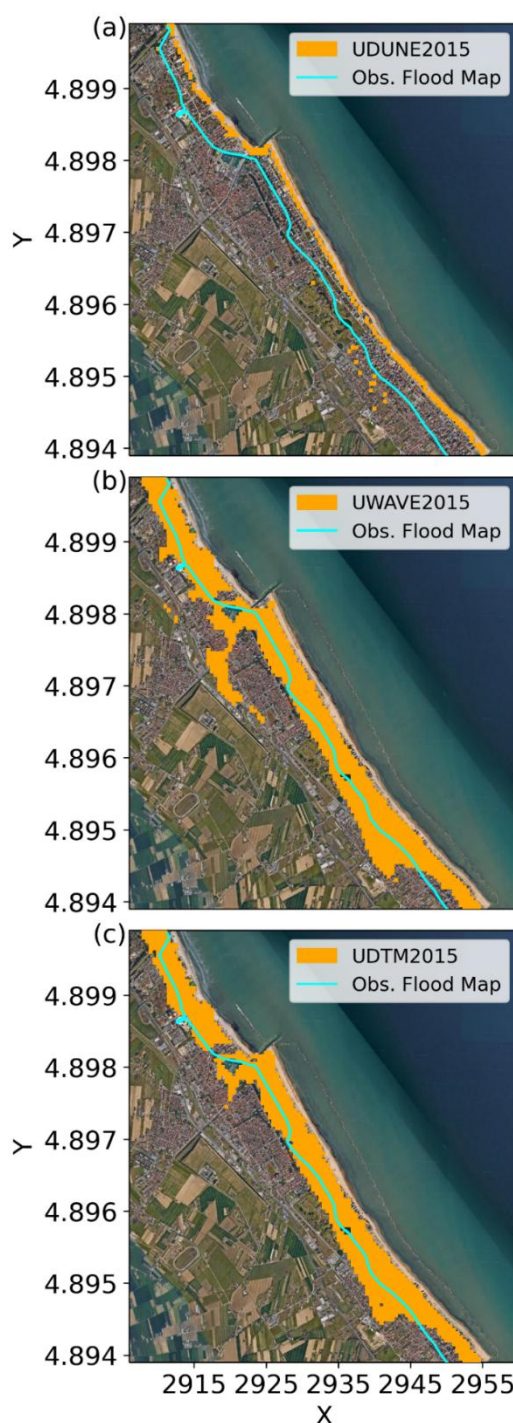


3.3 Effects of uncertainty

305 The uncertainty associated with the DTM (Figure 11c) and wave conditions (Figure 11b) exerts a significant influence on the extent of flooding observed in the simulations, whereas the uncertainty related to dune parameters is less pronounced for the 2015 event (Figure 11a). In the UDEM2015 simulations, discrepancies between the E2015 and E2015D scenarios are primarily confined to the cells of the portions of dunes that did not fail and areas with low water levels within the interior of the study domain (Figure 11a). Variations in the DTM critically affect the structural integrity of the dunes under storm conditions, leading to a more pronounced impact of DTM uncertainty. Specifically, in the E2015D+ simulation, no dune failures were observed, while the E2015D- simulation exhibited failures in 28 cells, corresponding to 22% of the dune structures. Consequently, the uncertainty area UDTM2015 is substantially larger compared to UDUNE2015. Notably, the flooded area in the E2015D- simulation was 1315% greater than that in E2015D+ and 7% greater than E2015D. The highest level of uncertainty was observed in UWAVE2015, where the flooded area accounting for the full swash (E2015DTWL) was 1463% larger than that using only the setup (E2015DWL). For both UWAVE2015 and UDEM2015, the largest discrepancies in flooded areas were directly linked to dune collapse. These findings highlight a strong nonlinearity in the relationship between flooded area and variations in the DTM and swash, with a critical threshold evident during the dune failure process.

310

315



320 **Figure 11: LISFLOOD-FP uncertainty associated with dunes UDUNE2015 (a), waves UWAVE2015 (b) and DTM UDTM2015 (c). Orange areas represent the uncertainty, given by the difference of flooded areas in the simulations. The cyan line corresponds to the limits of the observational flood map. © Google Maps**



For the 2022 event, the uncertainty associated with dunes (UDUNE2022; Figure 12a) has the most significant impact on the extent of flooding observed in the simulations since they did not fail. Specifically, the flooded area in the E2022 scenario is 1317% larger than that in E2022D. This is evident in Figure 9, which illustrates that dune integrity is maintained, thereby confining flooding to the beach strip. In contrast, the uncertainties associated with swash contribution and the Digital Terrain Model (UWAVE2022 and UDEM2022; Figure 12b) indicate no influence on dune collapses in this scenario. Consequently, the uncertainty for these parameters is negligible, with values effectively equal to zero.

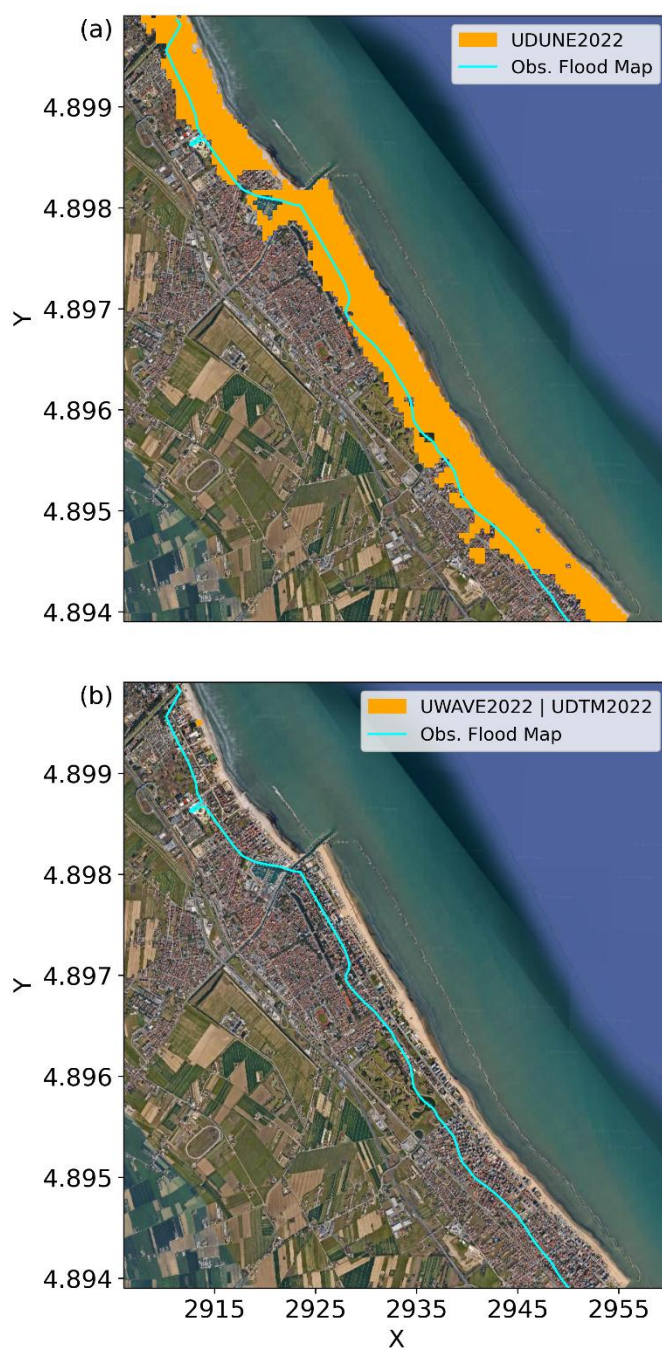


Figure 12: LISFLOOD-FP uncertainty associated with dunes UDUNE2022 (a), waves UWAVE2022 (b) and DTM UDTM2022 (c). Orange areas represent the uncertainty, given by the difference of flooded areas in the simulations. The cyan line corresponds to the limits of the observational flood map. © Google Maps



335 The analysis of the uncertainties reveals that during the 2015 event, where dune collapse occurred, the largest
source of uncertainty was associated with wave contributions, followed by uncertainties related to the Digital Terrain Model
(DTM) and dune parameters. These findings suggest that the failure of even a small number of dunes can produce flooding
conditions comparable to scenarios without dune protection, with the extent of flooding primarily influenced by water inflow
and the regional topography. Conversely, for the 2022 event, in which the dunes withstood the storm, uncertainties related to
340 the DTM, and swash contributions were insufficient to induce dune failure. This underscores the critical importance of dune
integrity in determining the simulation outcomes.

4 Discussion

345 The results from simulation E2015 provide valuable insights into the flooding dynamics of 2015 and demonstrate that
LISFLOOD-FP accurately reproduces inundation patterns for significant events by incorporating representations of dunes
and swash dynamics. The interaction between these protections, waves, and water levels can be complex, as demonstrated by
extreme events like the 2022 flood, when temporary dunes effectively safeguarded the shoreline, or the one of 2015, when
they failed. The model successfully predicted dune failure during the 2015 event, while in 2022, the dunes effectively
350 protected the land from inundation.

Our findings indicate that during the 2015 event, the swash significantly contributed to the erosion of these structures,
reaching up to 0.4 m in areas where dune collapse occurred (Figure 6d), ultimately allowing water to breach inland. Notably,
even though only a small portion of the dunes (5%) failed in our simulation, this was enough to trigger a flood as severe as if
no protections had been in place. Additionally, a possible outcome is that once a dune is breached, the remaining dunes may
355 obstruct the floodwater's backflow, worsening the aftermath of the inundation.

The event of 2022, when the dunes successfully protected the coast, is characterized by significantly lower values of the
swash than in 2015 (only 0.2 m, Figure 7c). For this event, representing the dunes was critical for improving the model's
accuracy, shifting the simulation bias from widespread overestimation of 739% to a modest underestimation.

360 The precise representation of the dune structures and the corresponding flooded areas depends heavily on accurate DTM
data and height measurements. Our uncertainty analysis, consistent with Dottori et al. (2022), shows that small changes in
DTM data can significantly enlarge flooded areas. This is a crucial point, as demonstrated by the 2015 event, where the
uncertainty in the DTM ranged from scenarios with no dune failure and minimal impact to a dam break scenario resulting in
a significant flood and highlights that frequent topographic surveys are essential for effective flood forecasts in the context of
disaster risk reduction.

365 Dune failure, like any coastal protection failure, is a stochastic process influenced by structural characteristics, natural
variability (e.g., erosion and sediment transport), and forcing mechanisms like water levels and wave action. While large-
scale assessments are limited by scarce high-resolution data, local-scale studies with detailed measurements of dune
geometry and maintenance practices can enhance predictive modeling.



Lateral boundary conditions at the coastline play a crucial role, particularly the inclusion of wave contributions for the
370 TWL. In the E2015DWL simulation, which neglects the swash and uses only the wave setup, the flood is confined to the
coast. Conversely, the E2015DTWL simulation, which accounts for the full swash contribution, extends the inundation
further inland. We found that E2015D, using an overwash efficiency $\alpha = 0.25$, provided a satisfactory representation of the
event. These findings highlight the importance of correctly representing the wave contribution to water supply: neglecting it
leads to underestimation, while using TWL as the boundary condition leads to overestimation. It is important to underline,
375 that in this study we set $\alpha = 0.25$ based on geometrical considerations and approximating the waves as triangular. But in
general, the overwash efficiency α can be used as a calibration parameter to best fit the simulation results.

Our results align with the findings of Zhang & Najafi (2020) and Carneiro-Barros et al. (2023), emphasizing the critical
interplay between various components of water levels. During the 2015 event (Figure 6), the storm surge peak coincided
with the peak of the waves, which were directed perpendicular to the shore. The occurrence of this event during neap tide,
380 combined with the peak of residuals during low tide, suggests that the tide did not exacerbate the event's intensity. This
implies that the impact would have been even more severe had it occurred during spring tide. In contrast, the 2022 event
(Figure 7) was less impactful, despite residuals reaching levels comparable to the 2015 event. This was because both surge
peaks coincided with low tide during spring tide, and the wave peak was not in phase with the storm surge, with mean wave
directions not perpendicular to the shore.

385 The occurrence of both events during low tide suggests that their severity could have been much greater, highlighting
the critical need for continuous monitoring of dune conditions and timely forecasting to ensure a comprehensive risk
management in Emilia Romagna.

The findings of this study also align with recent advancements in coastal flood modeling. Bertin et al. (2014) conducted
a comprehensive analysis of coastal flood risk using a full hydrodynamic model. Their findings highlighted the model's
390 remarkable ability to simulate coastal flood dynamics with high accuracy, emphasizing the critical role of detailed and
precise data on the geometry of coastal defenses. However, the study did not consider the potential defense failures, which
represents a significant limitation in understanding real-world flood risks. Additionally, while fully hydrodynamic models
are praised for their precision and reliability, their applicability is constrained by substantial computational demands, which
can hinder their use in large-scale or time-sensitive scenarios.

395 Closer to our approach, Leijnse et al., (2021) uses a shallow water equation model and incorporate a wave energy solver
which translate offshore wave conditions into nearshore dynamics. However, our method bypasses the computational
demands of a wave energy solver by directly integrating externally provided wave data. Geertsen et al. (2024) uses an
intermediate complexity model and integrated it with an empirical dike failure model using conditional FWD levels. In
contrast, our architecture is built inside the same code without the need to use separated models simplifying integration and
400 facilitating alternative and more complex failure scenarios developments. Our enhanced model offers a streamlined,
empirically grounded framework that maintains practical applicability without sacrificing detail.



The model's ability to represent the effects, failures, and drawbacks of coastal protection dunes, as well as quantify the contribution of waves, makes it a valuable tool for coastal hazard mapping. A possible way to overcome the limitation posed by the nonlinear nature of the uncertainty is using this LISFLOOD-FP in an ensemble framework. Additionally, this model can assist in defining appropriate failure heights for seasonal dunes in the region.

5 Conclusions

In this study, we improved the coastal flood modeling capabilities of LISFLOOD-FP by developing and testing new methods to account for the impact of waves, as well as the potential failure of coastal defenses due to overwash. Our findings demonstrate an improved ability to replicate accurately past inundation events, highlighting that incorporating dune failure and swash at the coastline are crucial modelling components for accurate coastal hazard mapping. This is especially important in regions like Emilia Romagna, where seasonal protective dunes are constructed and maintained annually to mitigate flood risk.

This improvement comes with an important caveat: the uncertainty regarding the exact topographic location and size of the temporary dunes, which are not captured in the available topographic data, propagates non-linearly in the extent of the simulated flood map. In our simulations, even a few centimeters of variation in dune height can be the determining factor between the collapse or survival of the dunes, significantly impacting the accuracy of flood predictions. This limitation is further compounded by the lack of observational flood maps, making it challenging to validate the model results. One potential way to address this issue in forecasting applications is by adopting an ensemble approach, which would allow for a more thorough probabilistic assessment of coastal hazards. By generating simulations with a variety of dune geometries and extreme sea level scenarios, this method could better capture the range of possible outcomes, helping to mitigate the uncertainty and improve the reliability of the hazard predictions. Furthermore, the implementation of such a strategy would be facilitated by the model's high computational efficiency.

Another way to partially solve the uncertainty conundrum is to design a monitoring system that would continuously observe the status of the dunes with drones or other cameras at appropriate locations. Present technology would allow this at a reasonable expense, and it will help to inform future data-driven modelling.

The findings represent a significant leap in the development of a coastal digital twin for coastal protection. The improved model can be a useful tool for coastal management by aiding in the prevention efforts of correctly sizing coastal defenses, leveraging on the existence of reliable statistics of extreme events. It can also contribute to disaster mitigation by effectively forecasting the occurrence and aftermath of extreme coastal events. By providing accurate simulations, the model can help in making informed decisions to protect coastal communities and infrastructure.



Data availability

435 The raw data supporting the conclusions of this article will be made available by the authors without undue reservation.

Author contributions

IRL conducted the conceptualization, software development, data elaboration and manuscript drafting. LM guided the supervision, conceptualization and manuscript drafting. LP supported with data provision, manuscript review, and revision. . GC contributed for the funding, manuscript review and revision. IF, SC, MV, MM and NP contributed with the manuscript
440 review and revision.

Competing interests

The authors have the following competing interests: Co-author Michalis Vousdoukas is employed by the company MV Coastal and Climate Research Ltd. Co-author Maurilio Milella is employed by the company Environmental Surveys S.r.l. The remaining authors declare that the research was conducted in the absence of any commercial or financial relationships
445 that could be construed as a potential conflict of interest.

Acknowledgements

This research has been supported by the European Space Agency (ESA) through the EOatSEE project, contract n° 4000138378/22/I-DT, under the Earth Observation Science for Society block of activities, part of the FutureEO-1 programme.

450 References

- Almarshed, B., Figlus, J., Miller, J., & Verhagen, H. J.: Innovative Coastal Risk Reduction through Hybrid Design: Combining Sand Cover and Structural Defenses. In *Journal of Coastal Research* (Vol. 36, Issue 1). <https://doi.org/10.2112/JCOASTRES-D-18-00078.1>, 2020.
- Armaroli, C., Ciavola, P., Perini, L., Calabrese, L., Lorito, S., Valentini, A., & Masina, M.: Critical storm thresholds for
455 significant morphological changes and damage along the Emilia-Romagna coastline, Italy. *Geomorphology*, 143–144. <https://doi.org/10.1016/j.geomorph.2011.09.006>, 2012.
- Armaroli, C., Duo, E., & Viavattene, C.: From Hazard to Consequences: Evaluation of Direct and Indirect Impacts of Flooding Along the Emilia-Romagna Coastline, Italy. *Frontiers in Earth Science*, 7. <https://doi.org/10.3389/feart.2019.00203>, 2019.



- 460 Bates, P. D., & De Roo, A. P. J.: A simple raster-based model for flood inundation simulation. *Journal of Hydrology*, 236(1–2). [https://doi.org/10.1016/S0022-1694\(00\)00278-X](https://doi.org/10.1016/S0022-1694(00)00278-X), 2000.
- Bates, P. D., Horritt, M. S., & Fewtrell, T. J.: A simple inertial formulation of the shallow water equations for efficient two-dimensional flood inundation modelling. *Journal of Hydrology*, 387(1–2). <https://doi.org/10.1016/j.jhydrol.2010.03.027>, 2010.
- 465 Bertin, X., Li, K., Roland, A., Zhang, Y. J., Breilh, J. F., & Chaumillon, E.: A modeling-based analysis of the flooding associated with Xynthia, central Bay of Biscay. *Coastal Engineering*, 94(212). <https://doi.org/10.1016/j.coastaleng.2014.08.013>, 2014
- Bessar, M. A., Choné, G., Lavoie, A., Buffin-Bélanger, T., Biron, P. M., Matte, P., & Anctil, F.: Comparative analysis of local and large-scale approaches to floodplain mapping: a case study of the Chaudière River. *Canadian Water Resources*
- 470 *Journal*, 46(4). <https://doi.org/10.1080/07011784.2021.1961610>, 2021.
- Carisi, F., Schröter, K., Domeneghetti, A., Kreibich, H., & Castellarin, A.: Development and assessment of uni- and multivariable flood loss models for Emilia-Romagna (Italy). *Natural Hazards and Earth System Sciences*, 18(7). <https://doi.org/10.5194/nhess-18-2057-2018>, 2018.
- Carneiro-Barros, J. E., Plomaritis, T. A., Fazeres-Ferradosa, T., Rosa-Santos, P., & Taveira-Pinto, F.: Coastal Flood
- 475 Mapping with Two Approaches Based on Observations at Furadouro, Northern Portugal. *Remote Sensing*, 15(21). <https://doi.org/10.3390/rs15215215>, 2023.
- Ciavola, P., Armaroli, C., Chiggiato, J., Valentini, A., Deserti, M., Perini, L., & Luciani, P.: Impact of storms along the coastline of Emilia-Romagna: The morphological signature on the Ravenna coastline (Italy). *Journal of Coastal Research, SPEC. ISSUE 50*. <https://doi.org/10.2112/jcr-si50-103.1>, 2007.
- 480 Ciavola, P., Perini, L., Luciani, P., Armaroli, C.: Il rilievo Lidar della costa dell'Emilia-Romagna: uno strumento per la valutazione dell'impatto delle mareggiate sulle zone costiere e per la caratterizzazione della morfodinamica delle spiagge. *HYDROGEO*, vol. 2006, p. 18-25, 2006.
- Didier, D., Baudry, J., Bernatchez, P., Dumont, D., Sadegh, M., Bismuth, E., Bandet, M., Dugas, S., & Sévigny, C.: Multihazard simulation for coastal flood mapping: Bathtub versus numerical modelling in an open estuary, Eastern Canada.
- 485 *Journal of Flood Risk Management*, 12(S1). <https://doi.org/10.1111/jfr3.12505>, 2019.
- Dottori, F., Alfieri, L., Bianchi, A., Skoien, J., & Salamon, P.: A new dataset of river flood hazard maps for Europe and the Mediterranean Basin. *Earth System Science Data*, 14(4). <https://doi.org/10.5194/essd-14-1549-2022>, 2022.
- Duo, E., Chris Trembanis, A., Dohner, S., Grottoli, E., & Ciavola, P.: Local-scale post-event assessments with GPS and UAV-based quick-response surveys: A pilot case from the Emilia-Romagna (Italy) coast. *Natural Hazards and Earth System*
- 490 *Sciences*, 18(11). <https://doi.org/10.5194/nhess-18-2969-2018>, 2018.
- European Environment Agency (EEA): *Economic losses from weather- and climate-related extremes in Europe*, 2023.
- European Environmental Agency (EEA): European Climate Risk Assessment. Executive summary. EEA Report 01/2024. In *The European Climate Risk Assessment (EUCRA)*, 2024.



- Harley, M. D., & Ciavola, P.: Managing local coastal inundation risk using real-time forecasts and artificial dune
495 placements. *Coastal Engineering*, 77. <https://doi.org/10.1016/j.coastaleng.2013.02.006>, 2013.
- IPCC: Summary for Policymakers. Global Warming of 1.5°C. An IPCC Special Report on the impacts of global warming of 1.5 °C above pre-industrial levels. In *Global Warming of 1.5°C. An IPCC Special Report on the impacts of global warming of 1.5°C above pre-industrial levels and related global greenhouse gas emission pathways, in the context of strengthening the global response to the threat of climate change*, 2018.
- 500 Le Gal, M., Fernández-Montblanc, T., Duo, E., Montes Perez, J., Cabrita, P., Souto Ceccon, P., Gastal, V., Ciavola, P., & Armaroli, C.: A new European coastal flood database for low-medium intensity events. *Natural Hazards and Earth System Sciences*, 23(11). <https://doi.org/10.5194/nhess-23-3585-2023>, 2023.
- Martinelli, L., Zanuttigh, B., & Corbau, C.: Assessment of coastal flooding hazard along the Emilia Romagna littoral, IT. *Coastal Engineering*, 57(11–12). <https://doi.org/10.1016/j.coastaleng.2010.06.007>, 2010.
- 505 Medvedev, I. P., Vilibić, I., & Rabinovich, A. B.: Tidal Resonance in the Adriatic Sea: Observational Evidence. *Journal of Geophysical Research: Oceans*, 125(8). <https://doi.org/10.1029/2020JC016168>, 2020.
- Melet, A., Meyssignac, B., Almar, R., & Le Cozannet, G.: Under-estimated wave contribution to coastal sea-level rise. *Nature Climate Change*, 8(3). <https://doi.org/10.1038/s41558-018-0088-y>, 2018.
- Mentaschi, L., Vousedoukas, M. I., García-Sánchez, G., Fernández-Montblanc, T., Roland, A., Voukouvalas, E., Federico, I.,
510 Abdolali, A., Zhang, Y. J., & Feyen, L.: A global unstructured, coupled, high-resolution hindcast of waves and storm surge. *Frontiers in Marine Science*, 10. <https://doi.org/10.3389/fmars.2023.1233679>, 2023.
- Nativi, Stefano., Craglia, Max., & Delipetrev, Blagoj: *Destination Earth: survey on “Digital Twins” technologies and activities, in the Green Deal area*. Publications Office of the European Union. <https://doi.org/10.2760/430025>, 2020.
- PERINI, L., CALABRESE, L., LORITO, S., & LUCIANI, P.: *Costal flood risk in Emilia-Romagna (Italy): the sea storm of February 2015*. <https://doi.org/10.5150/cmcm.2015.044>, 2015.
- 515 Pillai, U. P. A., Pinardi, N., Alessandri, J., Federico, I., Causio, S., Unguendoli, S., Valentini, A., & Staneva, J.: A Digital Twin modelling framework for the assessment of seagrass Nature Based Solutions against storm surges. *Science of the Total Environment*, 847. <https://doi.org/10.1016/j.scitotenv.2022.157603>, 2022.
- Shaw, J., Kesserwani, G., Neal, J., Bates, P., & Sharifian, M. K.: LISFLOOD-FP 8.0: The new discontinuous Galerkin
520 shallow-water solver for multi-core CPUs and GPUs. *Geoscientific Model Development*, 14(6). <https://doi.org/10.5194/gmd-14-3577-2021>, 2021.
- Shustikova, I., Neal, J. C., Domeneghetti, A., Bates, P. D., Vorogushyn, S., & Castellarin, A.: Levee breaching: A new extension to the LISFLOOD-FP model. *Water (Switzerland)*, 12(4). <https://doi.org/10.3390/W12040942>, 2020.
- Singhvi, A., Luijendijk, A. P., & van Oudenhoven, A. P. E.: The grey – green spectrum: A review of coastal protection
525 interventions. In *Journal of Environmental Management* (Vol. 311). <https://doi.org/10.1016/j.jenvman.2022.114824>, 2022.
- Smith, R. A. E., Bates, P. D., & Hayes, C. (2012). Evaluation of a coastal flood inundation model using hard and soft data. *Environmental Modelling and Software*, 30. <https://doi.org/10.1016/j.envsoft.2011.11.008>, 2012.



- Stockdon, H. F., Holman, R. A., Howd, P. A., & Sallenger, A. H.: Empirical parameterization of setup, swash, and runup. *Coastal Engineering*, 53(7). <https://doi.org/10.1016/j.coastaleng.2005.12.005>, 2006.
- 530 United Nations Office for Disaster Risk Reduction: The human cost of disasters: an overview of the last 20 years (2000-2019). In *Human Cost of Disasters*, 2020.
- van Rijn, L. C.: Prediction of dune erosion due to storms. *Coastal Engineering*, 56(4). <https://doi.org/10.1016/j.coastaleng.2008.10.006>, 2009.
- van Wiechen, P. P. J., de Vries, S., Reniers, A. J. H. M., & Aarninkhof, S. G. J.: Dune erosion during storm surges: A review
535 of the observations, physics and modelling of the collision regime. In *Coastal Engineering* (Vol. 186). <https://doi.org/10.1016/j.coastaleng.2023.104383>, 2023.
- Vousdoukas, M. I.: Erosion/accretion patterns and multiple beach cusp systems on a meso-tidal, steeply-sloping beach. *Geomorphology*, 141–142. <https://doi.org/10.1016/j.geomorph.2011.12.003>, 2012.
- Vousdoukas, M. I., Voukouvalas, E., Mentaschi, L., Dottori, F., Giardino, A., Bouziotas, D., Bianchi, A., Salamon, P., &
540 Feyen, L.: Developments in large-scale coastal flood hazard mapping. *Natural Hazards and Earth System Sciences*, 16(8). <https://doi.org/10.5194/nhess-16-1841-2016>, 2016.
- Wijnberg, K., Poppema, D., Mulder, J., van Bergen, J., Campmans, G., Galiforni-Silva, F., Hulscher, S., & Pourteimouri, P.: Beach-dune modelling in support of Building with Nature for an integrated spatial design of urbanized sandy shores. *Research in Urbanism Series*, 7. <https://doi.org/10.47982/rius.7.136>, 2021.
- 545 Williams, L. L., & Lück-Vogel, M.: Comparative assessment of the GIS based bathtub model and an enhanced bathtub model for coastal inundation. *Journal of Coastal Conservation*, 24(2). <https://doi.org/10.1007/s11852-020-00735-x>, 2020.
- Wilmink, R., McCall, R., Santen, R. Van, Kuik, N. van, Pluis, S., Bakker, A. de, & Steetzel, H.: XBEACH IMPLEMENTATION IN THE NEW NATIONAL COASTAL FLOOD RISK ASSESSMENT FRAMEWORK FOR THE DUTCH COAST. *Coastal Engineering Proceedings*, 37. <https://doi.org/10.9753/icce.v37.management.46>, 2023.
- 550 Zhang, Y., & Najafi, M. R.: Probabilistic Numerical Modeling of Compound Flooding Caused by Tropical Storm Matthew Over a Data-Scarce Coastal Environment. *Water Resources Research*, 56(10). <https://doi.org/10.1029/2020WR028565>, 2020.